

# **IDENTIFICATION OF NOVEL BACTERIAL MurA INHIBITORS**

by

**JoAnna Frances Shaw**

BA Biochemistry, New York University, 2016

Submitted to the Graduate Faculty of  
the Department of Infectious Diseases and Microbiology  
Graduate School of Public Health in partial fulfillment  
of the requirements for the degree of  
Master of Science

University of Pittsburgh

2018

UNIVERSITY OF PITTSBURGH

Graduate School of Public Health

This thesis was presented

by

**JoAnna Frances Shaw**

It was defended on

**April 18<sup>th</sup>, 2018**

and approved by

**Thesis Advisor:**

Nicolas Sluis-Cremer, PhD

Professor

Department of Medicine, Division of Infectious Diseases

School of Medicine

University of Pittsburgh

**Committee Members:**

Yohei Doi, MD, PhD

Associate Professor

Department of Medicine, Division of Infectious Diseases

School of Medicine

University of Pittsburgh

Jeremy Martinson, DPhil

Assistant Professor

Department of Infectious Diseases and Microbiology

Graduate School of Public Health

University of Pittsburgh

Copyright © by JoAnna F. Shaw

2018

## **IDENTIFICATION OF NOVEL BACTERIAL MurA INHIBITORS**

JoAnna F. Shaw, M.S.

University of Pittsburgh, 2018

### **ABSTRACT**

Antibiotic resistance is a persistent and serious public health issue which causes many illnesses and deaths per year. In contrast to the rapid increase and spread of drug-resistant bacteria, antibiotic development has slowed, and there is a clear need to identify and develop antibiotics with new scaffolds and mechanisms of action. In particular, there is a specific need for novel antimicrobial agents which are active against both gram negative and gram positive pathogens. The bacterial enzyme MurA catalyzes the transfer of enolpyruvate from phosphoenolpyruvate (PEP) to uridine diphospho-*N*-acetylglucosamine (UNAG), which is the first committed step of bacterial cell wall biosynthesis. Currently, the only antibiotic targeted toward MurA is fosfomycin, which inhibits MurA by forming a covalent bond with MurA's active site residue, Cys115. However, MurA variants which lack the cysteine residue in the active site (e.g. *M. tuberculosis* MurA and some vancomycin resistant *Enterococcus* (VRE) strains) are resistant to fosfomycin.

The goal of this study was to identify novel MurA inhibitors with a different mechanism of action than fosfomycin, and which are active against a range of gram negative and gram positive bacteria. To this end, we have developed and optimized an *in vivo* high-throughput screening assay to test recombinant MurA enzyme against the TimTec ApexScreen library, a drug library with 5,040 structurally diverse compounds. The hits identified from this screen were further validated using different assays, including bacterial growth curves. Minimum Inhibitory

Concentration (MIC) values were determined for the three most promising hits. Toxicity assays for these hits were also conducted in two cell lines. Future directions include further characterizing the mechanisms of action and testing for toxicity in other cell lines, including primary cells.

## TABLE OF CONTENTS

<b>PREFACE.....</b>	<b>XII</b>
<b>1.0 INTRODUCTION.....</b>	<b>1</b>
<b>1.1 ANTIBIOTIC RESISTANCE .....</b>	<b>1</b>
<b>1.1.1 Golden Era of Antibiotics .....</b>	<b>1</b>
<b>1.1.2 Emergence of Resistance.....</b>	<b>2</b>
<b>1.1.3 Causes of Antibiotic Resistance.....</b>	<b>3</b>
<b>1.2 WHO PRIORITY PATHOGENS .....</b>	<b>5</b>
<b>1.3 FOSFOMYCIN .....</b>	<b>6</b>
<b>1.3.1 Clinical Use.....</b>	<b>7</b>
<b>1.3.2 Resistance .....</b>	<b>7</b>
<b>1.4 MURA .....</b>	<b>8</b>
<b>2.0 SPECIFIC AIMS.....</b>	<b>11</b>
<b>2.1 PROJECT STATEMENT.....</b>	<b>11</b>
<b>2.2 PROJECT SPECIFIC AIMS.....</b>	<b>11</b>
<b>2.2.1 Specific Aim 1: To screen the TimTec® ApexScreen Library for potential MurA inhibitors. ....</b>	<b>11</b>
<b>2.2.2 Specific Aim 2: To characterize promising hits identified from the high-throughput screens.....</b>	<b>12</b>

<b>3.0</b>	<b>MATERIALS AND METHODS .....</b>	<b>13</b>
<b>3.1</b>	<b>RECOMBINANT PROTEIN EXPRESSION AND PURIFICATION .....</b>	<b>13</b>
<b>3.2</b>	<b>TIMTEC® APEXSCREEN DRUG LIBRARY .....</b>	<b>15</b>
<b>3.3</b>	<b>HIGH-THROUGHPUT SCREENING ASSAY: MALACHITE GREEN..</b>	<b>16</b>
<b>3.4</b>	<b>ARTEFACT SCREEN .....</b>	<b>19</b>
<b>3.5</b>	<b>MIC ASSAY .....</b>	<b>19</b>
<b>3.6</b>	<b>TOXICITY ASSAY .....</b>	<b>20</b>
<b>4.0</b>	<b>RESULTS .....</b>	<b>22</b>
<b>4.1</b>	<b>AIM 1: HIGH-THROUGHPUT SCREENS .....</b>	<b>22</b>
<b>4.1.1</b>	<b>Enzyme Purification .....</b>	<b>22</b>
<b>4.1.2</b>	<b>Primary and Secondary Screens .....</b>	<b>23</b>
<b>4.1.3</b>	<b>Artefact Screen .....</b>	<b>26</b>
<b>4.1.4</b>	<b><i>In vivo</i> screening*.....</b>	<b>27</b>
<b>4.2</b>	<b>AIM 2: INHIBITOR CHARACTERIZATION.....</b>	<b>30</b>
<b>4.2.1</b>	<b>MIC Assay .....</b>	<b>30</b>
<b>4.2.2</b>	<b>Toxicity Assays.....</b>	<b>34</b>
<b>4.2.3</b>	<b>Selectivity Indexes.....</b>	<b>37</b>
<b>5.0</b>	<b>DISCUSSION .....</b>	<b>38</b>
<b>5.1</b>	<b>ENZYME PURIFICATION.....</b>	<b>38</b>
<b>5.2</b>	<b>PRIMARY AND SECONDARY SCREENS.....</b>	<b>38</b>
<b>5.3</b>	<b>ARTEFACT SCREEN .....</b>	<b>39</b>
<b>5.4</b>	<b>MIC ASSAYS.....</b>	<b>39</b>
<b>5.5</b>	<b>TOXICITY ASSAYS.....</b>	<b>40</b>

5.5.1	HeLa cells .....	40
5.5.2	293T cells .....	41
5.5.3	Selectivity Indexes.....	41
6.0	CONCLUSIONS .....	43
7.0	PUBLIC HEALTH RELEVANCE .....	44
	BIBLIOGRAPHY .....	45

## LIST OF TABLES

Table 1. High-throughput screen hit rate. ....	30
Table 2. P22E7 average MIC values.....	32
Table 3. P24C4 average MIC values. ....	33
Table 4. P31A4 average MIC values. ....	33

## LIST OF FIGURES

Figure 1. Reaction catalyzed by MurA. ....	8
Figure 2. Fosfomicin is ineffective against bacteria with the Cys-Asp mutation in the MurA active site. ....	9
Figure 3. Half maximal inhibitory concentrations of fosfomicin acting on MurA. There is no difference in MurA activity of the C119D variant when exposed to very high levels of fosfomicin. ....	14
Figure 4. Before the reaction proceeds, all wells are yellow. ....	16
Figure 5. When the reaction proceeds, wells turn green. ....	16
Figure 6. Example plate with positive and negative controls in quadruplicate. ....	17
Figure 7. Plate map for high-throughput primary enzyme screen. ....	18
Figure 8. Example plate map for compound P24C4 MIC assay. ....	20
Figure 9. Example compound P24C4 toxicity assay plate map. ....	21
Figure 10. SDS-Page Gel confirming presence of purified MurA enzymes. ....	22
Figure 11. Representative plate from primary screen. ....	23
Figure 12. Representative heat map for VRE WT plate 43. ....	24
Figure 13. Representative heat map for VRE C119D plate 43. ....	24
Figure 14. Scatterplot of WT and C119D hits from plate 43 of the primary drug screen. ....	24
Figure 15. Representative daughter plate 12 from secondary drug screen. ....	25

Figure 16. Artefact assay, plate 1.....	26
Figure 17. Artefact assay control plate 1. ....	26
Figure 18. Artefact assay control plate 2. ....	26
Figure 19. Artefact assay, plate 2.....	26
Figure 20. Scatterplot of artefact screen data.....	27
Figure 21. Plate results for <i>in vivo</i> screening. Bacterial growth is shown in red, while non-growth in shown in green. ....	28
Figure 22. P22E7 IC <sub>50</sub> curve. ....	29
Figure 23. P24C4 IC <sub>50</sub> curve.....	29
Figure 24. P22E7 IC <sub>50</sub> curve. ....	29
Figure 25. P33A7 IC <sub>50</sub> curve. ....	29
Figure 26. Representative MIC results for compound P22E7. ....	31
Figure 27. Representative MIC results for compound P24C4.....	31
Figure 28. Representative MIC results for compound P31A4.....	32
Figure 29. HeLa incubated with [P31A4].....	34
Figure 30. HeLa incubated with [P24C4].....	34
Figure 31. HeLa incubated with [P22E7]. ....	34
Figure 32. HeLa incubated with DMSO controls. ....	34
Figure 33. 293T incubated with [P31A4]. ....	35
Figure 34. 293T incubated with [P24C4]. ....	35
Figure 35. 293T incubated with DMSO controls.....	36
Figure 36. 293T incubated with [P22E7].....	36

## **PREFACE**

Acknowledgements include my thesis advisory committee: Drs. Nicolas Sluis-Cremer, Yohei Doi, and Jeremy Martinson. I would also like to acknowledge contributions from various members and visiting scholars of the Sluis-Cremer and Doi labs including Adam Tomich, Yan (Grace) Guo, and Roberta Mettus.

## 1.0 INTRODUCTION

### 1.1 ANTIBIOTIC RESISTANCE

#### 1.1.1 Golden Era of Antibiotics

Penicillin was discovered accidentally in 1928 by Alexander Fleming, a Professor of Bacteriology at St. Mary's hospital in London (1). A derivative from the common bread mold *Penicillium*, it appeared as a green, fuzzy substance inhibiting *Staphylococcus* growth on an old petri dish. This chance observation, coupled with the successful isolation and mass-production of penicillin in the 1940s by Oxford researchers Sir Howard Florey and Ernst Chain, ushered in a new era of medicine, one in which minor cuts and scrapes, as well as serious infectious diseases such as diphtheria, pneumonia, and scarlet fever, no longer posed a potentially deadly threat to much of the developed world. Fleming, Florey, and Chain shared the 1945 Nobel Prize for Medicine as a result of their work (2, 3).

The "Golden Era" of antibiotic use and discovery had thus begun. In the period from the 1940s to the 1960s, researchers identified new antimicrobials mainly by screening soil-derived microbes, which led to the discovery of streptomycin, chloramphenicol, and many other antimicrobials (4, 5). In fact, about one-half of the antibiotics commonly used today in a clinical

setting were discovered within the period from 1950 to 1960 (6). No new classes of antibiotics have been discovered since the 1970s (7).

During the 20<sup>th</sup> century, deaths as a result of infectious diseases in the United States declined significantly, from 797 deaths per 100,000 in 1900 to 36 deaths per 100,000 in 1980 (8). The leading causes of death had shifted from infectious to chronic disease; in 1900, the top two causes of death were pneumonia and tuberculosis, while heart disease and cancer led mortality rates by 1997 (9). The control of infectious diseases evident throughout the 20<sup>th</sup> century can be attributed to many factors, including better sanitation and hygiene measures as well as vaccination, but the concurrent role of antibiotics and other antimicrobial measures cannot be understated (9). In World War II alone, penicillin saved thousands of wounded soldiers and civilians from dying of bacterial infections (10).

By the end of the 20<sup>th</sup> century, new challenges in public health had begun to emerge: human immunodeficiency virus (HIV) appeared, along with the emergence of drug-resistant tuberculosis. An overall increase in morbidity and mortality in the last twenty years of the century emphasized the ability of microbes to evolve, as well as the need for disease prevention methods of public health intervention which did not rely so heavily on antibiotic use alone (11).

### **1.1.2 Emergence of Resistance**

Antimicrobial resistance (AMR) occurs when microbes evolve upon exposure to antimicrobial agents, rendering them refractory to inhibition by the drug. Antibiotic resistance refers specifically to bacterial resistance against these drugs, though the terms are often used interchangeably.

Bacterial resistance to antimicrobials occurs in nature. Because many antibiotics are naturally-derived compounds (particularly those from the soil), it makes sense that some species of bacteria are intrinsically resistant to certain antibiotics due to evolutionary competition between microbes. Intrinsic resistance to penicillin, for example, was observed in 1940, shortly after its discovery and before widespread clinical use (12). However, the main focus of the public health problem of antimicrobial resistance is acquired resistance in a bacterial population which was originally susceptible to the antimicrobial compound (13).

Shortly after penicillin was introduced on a widespread clinical scale in the 1940s, acquired resistance began to emerge; so much so, that by the 1950s, many of the gains of the prior decade were threatened (14). In response, researchers discovered and deployed new beta-lactam antibiotics, and through the 1960s and early 1980s, the pharmaceutical industry introduced many new types of antibiotics to combat the growing resistance problem (15). However, in the early 1980s, the antibiotic pipeline began to dry up, with fewer new drugs being introduced to the public. Today, resistance has been seen to nearly all antibiotics that have been developed. With a lack of new antibiotics, as well as behavioral factors propagating resistance, bacterial infections have again become an urgent public health threat (10).

### **1.1.3 Causes of Antibiotic Resistance**

Indiscriminate antibiotic use in humans (both overuse and inappropriate prescribing) is a significant factor which adds to the selective pressure for bacteria to develop strategies to escape eradication, thus resulting in acquired resistance (16). Epidemiological studies have shown there is a direct relationship between antibiotic consumption and the emergence and dissemination of

resistant bacteria strains, while incorrect prescription of antibiotics exposes individual patients to potential complications of antibiotic therapy without any therapeutic benefit (17, 18).

Another contributing factor to antibiotic resistance is extensive agricultural use. Approximately 80% of the antibiotics sold in the United States are used for animal agriculture (19). It is common practice to feed animals a consistent, low dose of antibiotics to encourage weight gain and to prevent infections, in addition to using these drugs to treat serious infections and assist with surgical procedures in animals (20). This widespread use of antibiotics in livestock contributes—by means of natural selection—to the emergence of antimicrobial-resistant bacteria and has significant public health implications including environmental and food-borne transmission of resistant bacteria to humans, as well as transmission to agricultural workers via direct contact (21).

Lastly, few new antibiotics have been developed since the 1980s. To combat threats of resistance in the past, pharmaceutical companies had devoted resources to discovering new antimicrobial agents. However, due to both regulatory and economic hurdles, this strategy has been stalled. Economically, there is less financial incentive for pharmaceutical companies to pursue research of novel antibiotics. Because antibiotics are used for relatively short periods and are often curative, companies prefer to invest in more profitable drugs for chronic diseases such as diabetes and psychiatric disorders (22). The low cost, availability, and ease-of-use of antibiotics, combined with the desire of clinicians to use new drugs judiciously in a clinical setting leads to a diminished return on investment for these drugs as well, further disincentivizing pharmaceutical companies from pursuing novel antimicrobial research (23). Regulatory obstacles often include differences in clinical trial requirements among countries, changes in regulatory and licensing rules, and ineffective channels of communication (22). As a

result, due to a shortage of novel antimicrobial agents, many researchers are re-evaluating older antibiotics and their efficacy against a variety of both gram-negative and gram-positive pathogens (24, 25).

## **1.2 WHO PRIORITY PATHOGENS**

The World Health Organization (WHO) has determined that antibiotic resistance requires urgent, coordinated action at global, regional, and national levels (26) . The WHO has conducted an annual evaluation of the antibacterial clinical development pipeline, based on an in-depth analysis conducted by an advisory group of clinicians, microbiologists, and other antibiotic resistance experts. In this report, the organization lists twelve priority pathogens on which it believes research and development efforts should be focused.

The top WHO priority pathogen is tuberculosis (TB), caused by the gram negative - *Mycobacterium tuberculosis*. TB is the number one global infectious disease killer, causing nearly 2 million deaths per year (27). Drug-resistant TB is the most common and lethal airborne AMR disease worldwide today, causing 250,000 deaths per year (28). For multi-drug resistant TB, which includes strains of the disease resistant to first line treatments of both rifampin and isoniazid, disease burden and treatment outcome has been particularly difficult to improve (26). Other WHO critical priority pathogens include a mix of gram-negative and gram-positive pathogens, such as *Pseudomonas aeruginosa*, *Enterobacteriaceae*, vancomycin-resistant *Enterococcus faecium* (VRE), and *Staphylococcus aureus*.

Gram-negative bacteria currently pose a serious global threat to public health. However, there exists a clear and pressing need to develop new antimicrobials against gram positive

organisms as well. Multi-drug resistant gram-positive bacteria, including VRE and methicillin-resistant *S. aureus* (MRSA), as well as drug-resistant *S. pneumoniae* have been designated as serious public health threats by the US Centers for Disease Control and Prevention (CDC) (29). Both VRE and MRSA are common causes of bloodstream and other infections in hospitalized patients in the United States causing upwards of 12,000 deaths per year, and infections due to drug-resistant *S. pneumoniae* are estimated to cause approximately 7,000 deaths per year in the United States (29, 30). By focusing research efforts on developing or expanding the use of existing antibiotics which target both gram-negative and gram-positive organisms, we can target a greater range of resistant bacteria and maximize public health impact.

### **1.3 FOSFOMYCIN**

Fosfomycin is an old antibiotic, discovered from *Streptomyces* in 1969, and is effective against both gram-negative and gram-positive bacteria (31). It is highly active against extended spectrum  $\beta$ -lactamase (ESBL)-producing *E. coli*, with MIC<sub>50</sub> and MIC<sub>90</sub> values (minimum inhibitory concentrations that inhibit 50% and 90% of the isolates, respectively) generally falling between 2 and 4 mg/L (32). ESBL-producing bacterial strains are particularly feared as they are resistant to all penicillins, to cephalosporins (including third and fourth generation agents), and to aztreonam, and they are often cross-resistant to trimethoprim/sulfamethoxazole and quinolones as well (33).

Due to fosfomycin's broad spectrum antimicrobial activity, its effectiveness against MDR *E. coli*, and faced with a paucity of novel antibiotics, physicians have reconsidered it for use against a variety of both gram-negative and gram-positive MDR pathogens (32).

### 1.3.1 Clinical Use

Fosfomycin is commonly prescribed orally as a first-line treatment against uncomplicated urinary tract infections (UTIs), and functions as an inhibitor of the bacterial enzyme MurA (see Chapter 1.4). In a few European countries, fosfomycin is approved to be administered intravenously to treat soft-tissue infection and sepsis (34). As previously mentioned, fosfomycin is effective against several species of ESBL-producing bacteria, and because of this it has been used in clinical trials in combination with other antimicrobials to successfully treat nosocomial infections caused by ESBL-producing carbapenem-resistant *K. pneumoniae* (35).

### 1.3.2 Resistance

Though fosfomycin is highly effective against ESBL-producing *E. coli*, its susceptibility is decreased in some other species of MDR bacteria. In ESBL-producing carbapenem-resistant *K. pneumoniae*, the MIC<sub>50</sub> and MIC<sub>90</sub> values are significantly higher than in *E. coli* (~32 mg/L and ~128 mg/L, respectively), translating to susceptibility rates of ~ 80%. Data on other species are scarce, but *Enterobacter* spp., *Proteus* spp. and *P. aeruginosa* have susceptibility rates of ~ 70% (36, 37).

The most clinically relevant mechanism of fosfomycin resistance involves expression of FosA3, an enzyme which catalyzes the Mn<sup>2+</sup>- and K<sup>+</sup>-dependent glutathione-mediated degradation of fosfomycin (38). Epidemiologically this enzyme was initially identified in Japan but has subsequently been shown to be widespread in East Asia in ESBL-producing *E. coli* and less commonly in *K. pneumoniae* from humans (38, 39). The FosA3 enzyme confers intrinsic

resistance in some species of bacteria, and the *fosA3* gene can also spread plasmid-mediated resistance among different species in the *Enterobacteriaceae* family (38).

Other resistance mechanisms to fosfomycin, including intrinsic resistance observed in VRE isolates at the University of Pittsburgh Medical Center (UPMC) involve its target, the bacterial enzyme MurA (40).

#### 1.4 MurA

UDP-*N*-acetylglucosamine enolpyruvyl transferase (MurA) is a bacterial enzyme which catalyzes the transfer of enolpyruvate from phosphoenolpyruvate (PEP) to uridine diphospho-*N*-acetylglucosamine (UNAG), the first committed step of bacterial cell wall biosynthesis (Figure 1) (41). Fosfomycin is currently the only antibiotic which targets MurA, and functions by forming a covalent bond with the Cysteine115 residue in the active site of MurA, thereby inhibiting its function and resulting in bacterial cell death (Figure 2) (34).

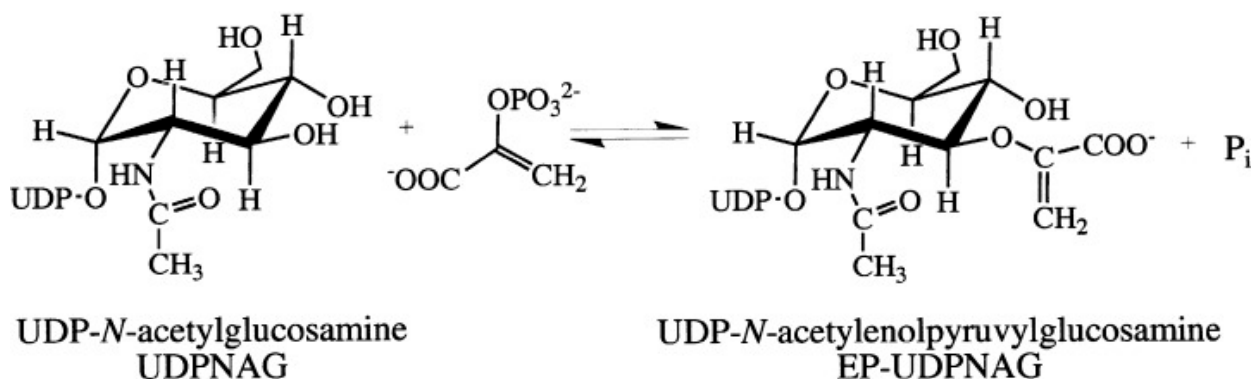


**Figure 1.** Reaction catalyzed by MurA.

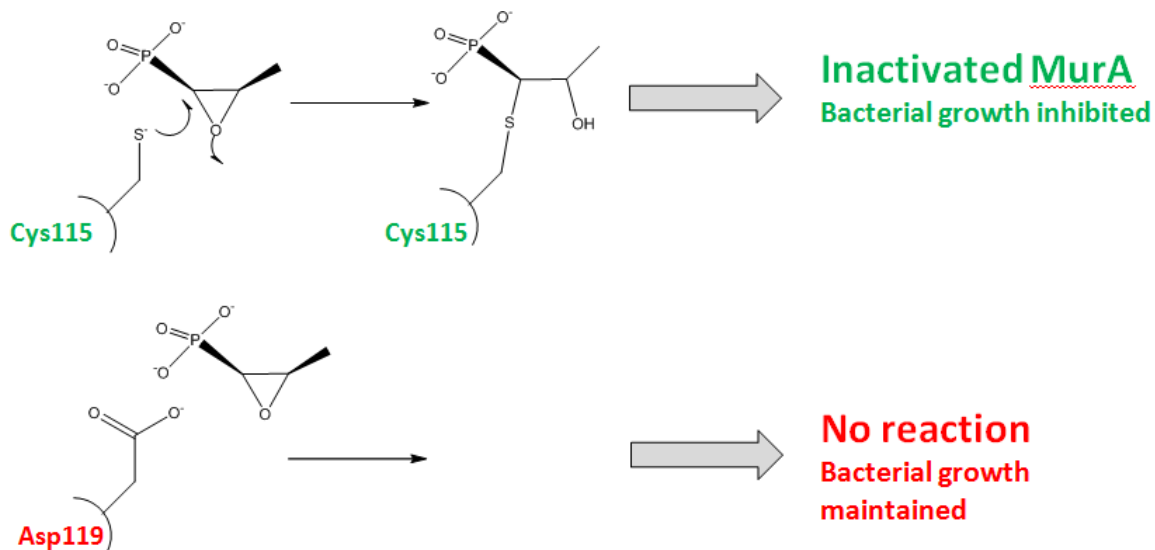


**Figure 2.** Fosfomicin is ineffective against bacteria with the Cys-Asp mutation in the MurA active site.

MurA variants which lack this cysteine residue in the active site are intrinsically resistant to fosfomicin. These species include *M. tuberculosis* and *B. burgdorferi*, which encode an Aspartate residue in place of Cys115 in the MurA active site. Previously mentioned VRE isolates discovered at UPMC also possess an Asp residue in place of the Cys115 in the active site of MurA (40).

Fosfomicin is ineffective against bacteria with the Cysteine-to-Aspartate amino acid change within the MurA active site. However, MurA is an extremely ubiquitous enzyme, and is highly conserved among bacteria, is essential for cell survival, and has no human homolog, all of which make it a desirable drug target (42). Therefore, identifying a MurA inhibitor that is active against both intrinsically fosfomicin-resistant MurA and fosfomicin-susceptible variants – which include WHO priority pathogens such as *M. tuberculosis* - is a logically sound research pursuit.

The goal of this study was to identify novel MurA inhibitors which have a different mechanism of action than fosfomycin, and which are active against a range of gram negative and gram positive bacteria. With luck, these novel inhibitors will serve as an antimicrobial agent that is clinically effective against both fosfomycin-sensitive and fosfomycin-resistant bacteria.

To that end, we purified two primary enzymes: VRE WT MurA, which contains the conserved Cys115 residue in the active site, and VRE C119D MurA, which contains an Asp residue at position 119. Using an *in vivo* high-throughput screen, we screened both enzymes against the TimTec® ApexScreen library, which contains 5,040 structurally diverse compounds, in search of a drug which inhibits both the wildtype and C119D substitution forms of MurA. Because these overlap hits inhibit both variants of the MurA enzyme, they likely have a different mechanism of action than fosfomycin, which exclusively targets Cys115 in wildtype MurA, and therefore may be useful compounds in expanding the clinical use of fosfomycin. After identifying these overlap hits, their inhibitory activity was further validated using bacterial growth curves, toxicity assays, and other methods.

## **2.0 SPECIFIC AIMS**

### **2.1 PROJECT STATEMENT**

The use of high-throughput screens for antibiotic drug discovery is not a novel concept; however it still remains a highly useful technique in the age of antibiotic resistance. This project uses high-throughput screens to sift through the TimTec® ApexScreen library of over 5,000 compounds to find a bacterial MurA enzyme inhibitor, which may eventually be used to replace or expand the use of fosfomycin in the clinical setting. The overall goal of this project is to identify and characterize an inhibitor(s) with a different mechanism of action than fosfomycin, so that bacterial species with intrinsic resistance to fosfomycin may be potential targets.

### **2.2 PROJECT SPECIFIC AIMS**

**2.2.1 Specific Aim 1:** To screen the TimTec® ApexScreen Library for potential MurA inhibitors.

- A. Using malachite-green based assays, primary and secondary screens were performed on the TimTec® ApexScreen Library. Results were quantified by spectroscopy and analyzed in Microsoft Excel.

- B.** An artefact screen using malachite green was also performed on remaining hits. Results were quantified by spectroscopy.

**2.2.2 Specific Aim 2:** To characterize promising hits identified from the high-throughput screens.

- A.** MIC assays were performed by incubating various species of bacteria with a given inhibitor for 24 hours. Results were quantified visually.
- B.** Toxicity assays were performed by incubating various concentrations of inhibitor with both HeLa and 293T HEK cell lines for 24 hours. Results were quantified by luminescence spectroscopy.

### **3.0 MATERIALS AND METHODS**

#### **3.1 RECOMBINANT PROTEIN EXPRESSION AND PURIFICATION**

VRE isolates were obtained from patients via rectal screening at the University of Pittsburgh Medical Center, Pittsburgh, PA, USA. 890 of these isolates were screened for resistance to fosfomycin, and 4 of these isolates had MICs  $>1024\mu\text{g/mL}$  for fosfomycin, indicating resistance. After amplification and sequencing it was determined that these isolates possessed a Cys119Asp (C119D) substitution in the active site of MurA. The half-maximal inhibitory concentrations ( $\text{IC}_{50}$ ) of fosfomycin for both WT and C119D were determined as well as other kinetic parameters (40). There is no difference in MurA activity of the C119D variant when exposed to very high levels of fosfomycin, while the wildtype Cys115 variant remains sensitive (Figure 3).

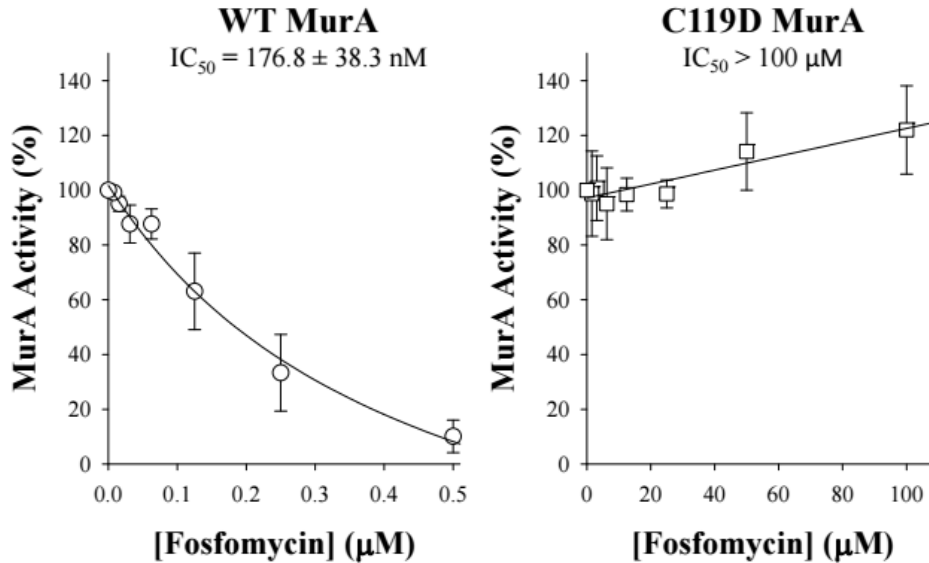


**Figure 3.** Half maximal inhibitory concentrations of fosfomycin acting on MurA. There is no difference in MurA activity of the C119D variant when exposed to very high levels of fosfomycin.

VRE WT, VRE C119D, and *M. tuberculosis murA* genes were synthesized (Genscript, Piscataway, NJ, USA) and cloned into a pE-SUMOstar prokaryotic expression system (LifeSensors, Malvern, PA, USA), and transformed into BL21 (DE3) pLysS competent *E. coli* cells with small-ubiquitin-related modifier (SUMO) and His<sub>6</sub> fusion tags. The hexahistidine SUMO fusion construct has been shown to enhance expression and facilitate purification with Ni-NTA chromatography, particularly with difficult-to-express proteins, when compared to traditional gene fusion systems (43). Transformed *E. coli* were grown overnight at 37 deg Celsius in Power Prime Broth with 100mg/L ampicillin. Overnight cultures were diluted 1:50 in fresh Power Prime broth, and grown to an optical density (OD) of 0.3 measured at 600nm before expression was induced for four hours using 1mmol/L isopropyl β-D-1-thiogalactopyranoside (IPTG). After expression, cells were obtained by centrifugation and resuspension in 50mmol/L

sodium phosphate buffer with protease inhibitor, and then lysed mechanically using a French press.

Cell supernatants were mixed with TALON Metal Affinity Resin (Clontech Laboratories, Inc., Mountain View, CA, USA), loaded into a gravity flow column, and washed with sodium phosphate buffer plus 0.3mol/L NaCl and 1 mmol/L  $\beta$ -mercaptoethanol. Bound protein was eluted with 100 mmol/L sodium phosphate containing 0.6mol/L NaCl, 240mmol/L imidazole, and 1 mmol/L  $\beta$ -mercaptoethanol. The protein was exchanged into 25 mmol/L Tris-HCl by using an NAP-25 column (GE Healthcare, Chicago, IL, USA). Protein concentration was determined with a Bradford assay with bovine serum albumin (BSA) as the standard. Purification was evaluated with a sodium dodecyl sulfate polyacrylamide gel electrophoresis (SDS-PAGE) gel. *M. tuberculosis* yield was too low to proceed, but the VRE WT and C119D variants had robust yields. The VRE purified proteins were then aliquoted and stored in 25% Glycerol at -80 deg Celsius for later use.

### **3.2 TIMTEC® APEXSCREEN DRUG LIBRARY**

The TimTec® ApexScreen drug library (TimTec, Inc., Newark, DE, USA) was selected due to its diversity and quantity of structurally active compounds. Each compound in this library obeys the Lipinski Rule of Five indicating a likelihood to display good oral bioavailability, solubility, and permeability profiles (44).

### 3.3 HIGH-THROUGHPUT SCREENING ASSAY: MALACHITE GREEN

The reaction catalyzed by MurA results in the production of UDP-*N*-acetylpyruvylglucosamine and free inorganic phosphate (Figure 1). The primary assay used in the high-throughput screen is the Malachite Green Phosphate Assay Kit (BioAssay Systems, Hayward, CA, USA), a colorimetric 96-well assay which changes color in the presence of free inorganic phosphate in solution. When the MurA reaction proceeds, inorganic phosphate is produced, and a color change occurs from yellow to green. When the MurA reaction is inhibited, inorganic phosphate is not produced and the color of the reagent remains yellow (Figures 4 and 5).

	2	3	4	5	6	7	8	9	10	11
A	Yellow									
B	Yellow									
C	Yellow									
D	Yellow									
E	Yellow									
F	Yellow									
G	Yellow									
H	Yellow									

**Figure 4.** Before the reaction proceeds, all wells are yellow.

	2	3	4	5	6	7	8	9	10	11
A	Green	Green	Green	Yellow	Green	Green	Green	Green	Green	Green
B	Green	Green	Green	Green	Green	Green	Yellow	Green	Green	Green
C	Green	Green	Green	Green	Green	Green	Green	Green	Green	Green
D	Green	Yellow	Green	Green	Green	Green	Green	Green	Green	Green
E	Green	Green	Yellow	Green	Green	Green	Green	Green	Green	Green
F	Green	Green	Green	Green	Green	Green	Yellow	Green	Green	Green
G	Green	Green	Green	Green	Green	Green	Green	Green	Green	Green
H	Green	Green	Green	Green	Green	Green	Green	Green	Green	Green

**Figure 5.** When the reaction proceeds, wells turn green.

1 $\mu$ L of each TimTex ApexScreen compound per well was incubated with PEP, UNAG, and enzyme in 96-well plates, and the reaction was quenched after 20 minutes as per the manufacturer recommendation. Enzyme and no-enzyme controls were also prepared with DMSO instead of drug in each plate (Figure 5). In total, 63 VRE WT plates were screened and 63 VRE C119D plates were screened in parallel during the primary screen for both enzymes.

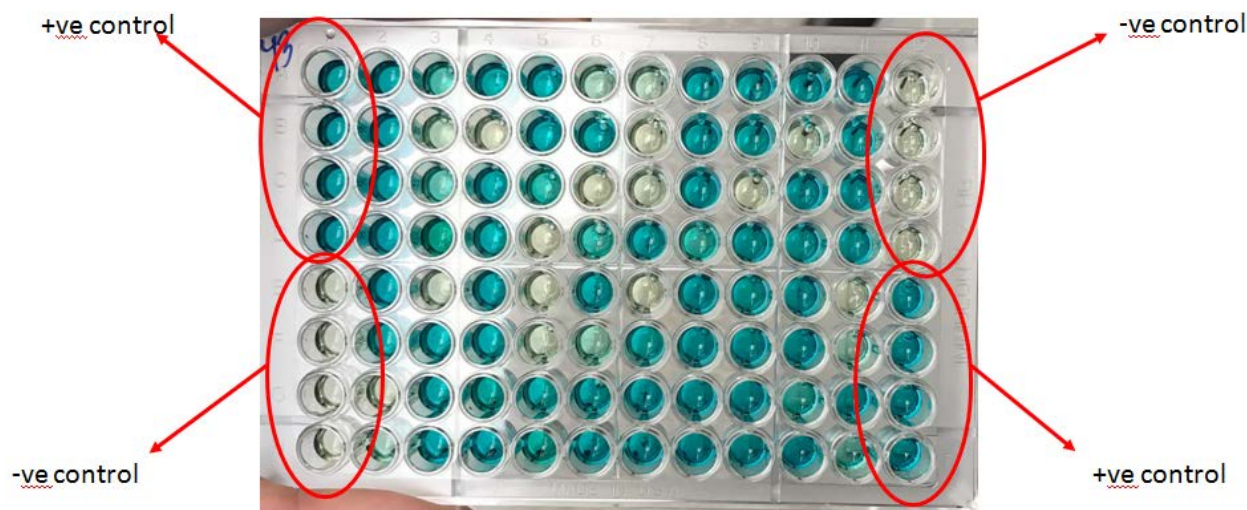


**Figure 6.** Example plate with positive and negative controls in quadruplicate.

The malachite green color change allowed for visual determination whether the MurA reaction was proceeding in each well of a 96-well plate (Figure 6). Absorption spectroscopy was also used to quantify the amount of free inorganic phosphate in solution. This data was imported into Microsoft Excel. Absorption data was scaled from 0 to 1 based on enzyme and no-enzyme controls, and a “Heat Map Analysis” was constructed to more easily compare data between plates. The criteria for a hit was 70% or greater reaction inhibition (phosphate absorption values from 0.000 to 0.300 out of 1.000).

	1	2	3	4	5	6	7	8	9	10	11	12
A	Compound-, MurA+	C1	C2	C3	C4	C5	C6	C7	C8	C9	C10	Compound-, MurA- (NO ENZYME)
B		C11	C12	C13	C14	C15	C16	C17	C18	C19	C20	
C		C21	C22	C23	C24	C25	C26	C27	C28	C29	C30	
D		C31	C32	C33	C34	C35	C36	C37	C38	C39	C40	
E	Compound-, MurA- (NO ENZYME)	C41	C42	C43	C44	C45	C46	C47	C48	C49	C50	Compound-, MurA+
F		C51	C52	C53	C54	C55	C56	C57	C58	C59	C60	
G		C61	C62	C63	C64	C65	C66	C67	C68	C69	C70	
H		C71	C72	C73	C74	C75	C76	C77	C78	C79	C80	

**Figure 7.** Plate map for high-throughput primary enzyme screen.

A drawback of the malachite green assay is its sensitivity to bubbles in each well, which may result in a false-positive hit reading as a result of natural variation in pipetting technique. To eliminate these potential false-positive hits, the VRE WT enzyme underwent a secondary screening using the same assay technique, and any hits not validated by the second screen were eliminated.

For the C119D enzyme, which resulted in a much smaller number of primary hits, primary hits were screened for pan-assay interference compounds (PAINs) using the BadApple scoring database. PAINs are molecules which are known to indiscriminately bind to substrate and result in false-positives in drug-screening (45). Once the PAINs molecules were eliminated, the WT and C119D results were compared in order to identify overlap hits, which were then further screened using an artefact assay.

### 3.4 ARTEFACT SCREEN

The artefact assay also implemented malachite green. Potential hits were incubated with pyrophosphate and no enzyme; absorption data was collected at 620nm and any wells with a reduction in absorption were considered artefacts and eliminated from consideration.

### 3.5 MIC ASSAY

The Minimum Inhibitory Concentration (MIC) is defined as the lowest concentration of an antimicrobial that will inhibit the visible growth of a microorganism after overnight incubation (46). MICs for remaining hits were conducted in 96-well plates with four bacterial strains: wildtype vancomycin resistant *Enterococcus faecium*, vancomycin resistance *Enterococcus faecium* with the C119D substitution, *Staphylococcus aureus*, and *Escherichia coli*. Both the *S. aureus* and *E. coli* are commercially available strains and were used as controls. Bacteria were incubated with fosfomycin, inhibitor, or DMSO overnight at a range of concentrations (Figure 7). Growth in each well was visually determined the following day.

		1	2	3	4	5	6	7	8	9	10	11	12
	Fosfomycin (ug/mL)	0	1	2	4	8	16	32	64	128	256	512	1024
	P24C4 (ug/mL)	0	0.08	0.16	0.31	0.63	1.25	2.5	5	10	20	40	80
A	VREWT + Fosfomycin												
B	VREWT + P31A4												
C	VREWT + DMSO												
D	C119D + Fosfomycin												
E	C119D + P31A4												
F	C119D + DMSO												
G													
H													

		1	2	3	4	5	6	7	8	9	10	11	12
	Fosfomycin (ug/mL)	0	1	2	4	8	16	32	64	128	256	512	1024
	P24C4 (ug/mL)	0	0.08	0.16	0.31	0.63	1.25	2.5	5	10	20	40	80
A	SA 25923 + Fosfomycin												
B	SA 25923 + P31A4												
C	SA 25923 + DMSO												
D	EC 25922 + Fosfomycin												
E	EC 25922 + P31A4												
F	EC 25922 + DMSO												
G													
H													

**Figure 8.** Example plate map for compound P24C4 MIC assay.

### 3.6 TOXICITY ASSAY

Toxicity assays on remaining hits were conducted using 96-well plates with two different cell lines. Standard cell culture methods were used to grow TZM-bl HeLa cells as well as 293T Human Embryonic Kidney (HEK) cells. For each assay, approximately 180µL of Dulbecco's Modified Eagle Medium (DMEM) containing approximately 20,000 cells per well was incubated at 37 deg Celsius with 20µL of inhibitor, DMSO control, or media control at varying

concentrations (Figure 8). After 24 hours of incubation, each well received 100 $\mu$ L of CellTiter-Glo<sup>®</sup> Luminescent Cell Viability Assay reagent (Promega, Madison, WI, USA) as per manufacturer recommendation. The CellTiter-Glo<sup>®</sup> assay determines the number of viable cells in culture based on quantitation of ATP (47). Luminescence was quantified via spectroscopy.

		1	2	3	4	5	6
P24C4 (ug/mL)	A	1.85	5.56	16.67	50	150	10% DMSO
	B	1.85	5.56	16.67	50	150	
P31A4 (ug/mL)	C	0.21	0.62	1.85	5.556667	16.67	
	D	0.21	0.62	1.85	5.556667	16.67	
P22E7 (ug/mL)	E	0.21	0.62	1.85	5.556667	16.67	Media Only
	F	0.21	0.62	1.85	5.556667	16.67	
DMSO	G	0.01%	0.03%	0.10%	0.31%	0.93%	
	H	0.01%	0.03%	0.10%	0.31%	0.93%	
10% DMSO gets 20uL DMSO instead of drug, Media only gets 20uL media instead of drug							

**Figure 9.** Example compound P24C4 toxicity assay plate map.

## 4.0 RESULTS

### 4.1 AIM 1: HIGH-THROUGHPUT SCREENS

#### 4.1.1 Enzyme Purification

VRE WT, C119D, and *M. tuberculosis* (TB) MurA enzymes were purified using standard methods as described in Chapter 3. An SDS-PAGE gel was run to confirm presence of purified protein (Figure 10). The molecular weights of VRE WT and C119D enzymes are ~44kD, and the molecular weight of TB MurA is ~47.4kD. The weak bands in the TB column contrast with the robust bands for both WT and C119D MurA. VRE WT and C119D MurA enzymes were stored in 50% glycerol at -80 deg C.

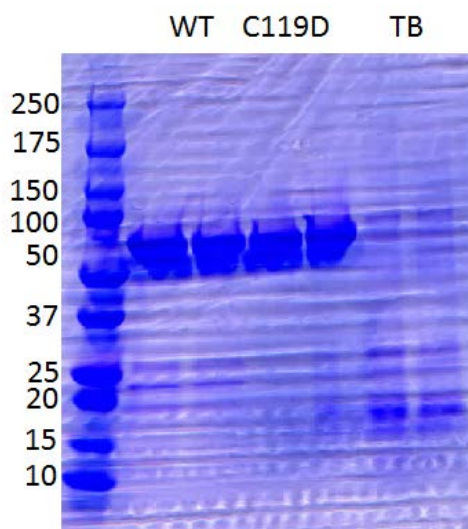


**Figure 10.** SDS-Page Gel confirming presence of purified MurA enzymes.

### 4.1.2 Primary and Secondary Screens

Enzymes were screened against the library of potential inhibitors using a malachite-green assay (as described, along with a plate map, in Chapter 3). Potential hits were validated by a secondary screen. Data from a representative plate (Plate 43 out of 63 plates in the primary screen) is shown here for brevity.



**Figure 11.** Representative plate from primary screen.

Figure 10 illustrates a representative plate from the primary drug library screen. The dark green wells represent reactions which have proceeded fully, while the yellow wells represent a potential MurA inhibition reaction. The uppermost left four and lowermost right four wells represent positive controls where we expect the enzymatic reaction to proceed fully, while the lowermost right four and uppermost left four wells are the negative controls without enzyme, where we expect no reaction to occur. Each of these plates was read at 620nm on a spectrophotometer to quantify the reaction in each well, and these readings were standardized on a scale from 0 to 1 to generate a color-coded heat map on Microsoft Excel, and to more easily compare data between plates.

The VRE WT and C119D MurA enzymes were concurrently screened against the drug library, and a heat map was created for each plate in the screens. A representative heat map of VRE WT Plate 43 can be seen in Figure 11, while a heat map for C119D MurA can be seen in Figure 12. Figure 13 is a scatterplot of the WT and C119D plate 43 screening data.

	2	3	4	5	6	7	8	9	10	11
A	0.898	0.394	1.000	0.987	0.131	0.086	0.924	1.000	0.933	0.986
B	0.988	0.103	0.009	0.968	0.977	0.006	1.000	0.805	0.049	0.819
C	1.000	0.316	1.000	0.499	0.009	0.039	1.000	0.008	1.000	1.000
D	1.000	1.000	0.790	0.004	0.611	0.941	0.448	1.000	0.767	0.879
E	1.000	0.031	1.000	0.013	1.000	0.000	1.000	0.833	1.000	0.022
F	0.633	0.807	0.808	0.034	0.183	0.639	1.000	0.981	1.000	0.153
G	0.000	0.880	1.000	0.723	0.998	1.000	0.981	1.000	0.446	0.939
H	0.110	0.924	0.948	0.763	1.000	1.000	1.000	0.994	1.000	0.302

**Figure 12.** Representative heat map for VRE WT plate 43.

	2	3	4	5	6	7	8	9	10	11
A	0.233	0.000	0.376	0.000	0.943	0.012	0.048	0.000	0.512	0.349
B	0.399	0.006	0.006	0.000	0.154	0.454	0.554	0.000	0.000	0.427
C	0.034	0.204	0.120	0.000	0.042	0.000	0.000	0.000	0.121	0.183
D	1.000	1.000	1.000	0.000	1.000	1.000	1.000	0.000	0.000	1.000
E	0.000	0.943	1.000	1.000	0.000	0.000	1.000	0.810	0.000	0.000
F	1.000	1.000	1.000	0.000	1.000	1.000	0.971	0.999	0.000	0.965
G	1.000	0.872	1.000	0.000	1.000	0.000	0.000	0.868	1.000	0.000
H	0.000	1.000	0.000	0.000	0.000	1.000	0.000	0.920	0.000	0.962

**Figure 13.** Representative heat map for VRE C119D plate 43.

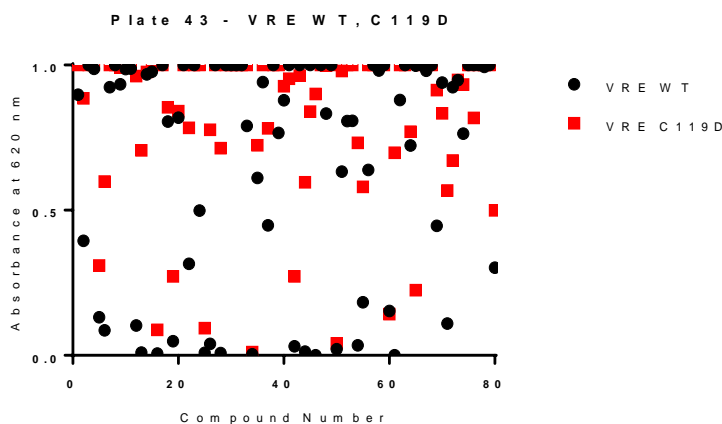


**Figure 14.** Scatterplot of WT and C119D hits from plate 43 of the primary drug screen.

The primary drug screen for the VRE WT MurA generated over 910 hits, which is an unfeasible number of molecular interactions to characterize within the scope of this study. Therefore, a secondary screen was carried out to validate the initial WT hits. Daughter plates were created from the hits of the original drug library, and another series of malachite green assays were performed. A representative plate (plate 12 out of 12 WT daughter plates) is shown in Figure 14. The green wells indicate reactions which have generated inorganic phosphate, while the yellow-orange wells indicate reactions which did not produce inorganic phosphate.

	2	3	4	5	6	7	8	9	10	11
A	1.000	0.885	1.000	1.000	0.309	0.599	1.000	1.000	0.992	1.000
B	1.000	0.962	0.706	0.976	0.997	0.088	1.000	0.855	0.272	0.841
C	1.000	0.784	1.000	1.000	0.094	0.777	1.000	0.714	1.000	1.000
D	1.000	1.000	1.000	0.012	0.724	1.000	0.782	1.000	1.000	0.927
E	0.953	0.272	0.964	0.596	0.840	0.901	1.000	0.998	1.000	0.041
F	0.980	1.000	1.000	0.732	0.581	1.000	1.000	0.999	1.000	0.142
G	0.698	1.000	1.000	0.770	0.224	1.000	1.000	1.000	0.914	0.834
H	0.568	0.671	0.949	0.933	1.000	0.818	1.000	1.000	1.000	0.499

**Figure 15.** Representative daughter plate 12 from secondary drug screen.

After the secondary WT screen, 775 hits were validated, and the hit rate was reduced from 18.06% to 15.38%. The number of C119D primary screen hits was 182, with an initial hit rate of 3.6%. After the primary C119D hits were identified, they were cross-checked against the BadApple scoring system database to eliminate PAINs (see Chapter 3), which reduced the C119D hit rate from 3.6% to 1.2%, a much more feasible number of compounds to further analyze. At this point, 128 hits from the WT and C119D screens were determined to be overlaps, and the overall hit rate between the two enzymes was 2.54%.

### 4.1.3 Artefact Screen

To screen for artefacts, the overlap hits were incubated in 96-well plates with deionized water and pyrophosphate, but with no enzyme. Because the enzyme was not present in any wells, any compound which disrupted the pyrophosphate signal was determined to be an artefact and eliminated from further consideration. Pyrophosphate was measured via spectrophotometer at 620nm. Signal disruption criteria was determined to be any well with a signal of less than 1.000.

0.757	0.824	0.594	0.654	0.900	0.670	0.664	0.560	0.572	0.502	0.522	0.495
0.457	0.321	0.574	0.800	0.808	0.457	0.628	0.604	0.523	0.510	0.607	0.614
0.530	0.418	1.020	0.498	0.561	0.564	0.704	0.515	0.398	0.567	0.549	0.552
0.477	0.335	0.442	0.497	0.948	1.238	0.848	0.550	0.488	1.060	0.734	0.753
0.534	0.355	0.646	0.335	0.401	0.515	0.606	0.411	0.436	0.565	0.500	0.504
0.573	0.631	1.000	0.585	0.572	0.343	0.499	0.684	0.695	0.448	0.518	0.504
0.507	0.316	1.036	0.308	0.429	1.309	0.526	1.151	0.766	0.522	0.867	0.900
0.483	0.653	0.311	0.508	0.555	0.453	0.454	0.745	0.370	0.320	0.434	0.424

Figure 16. Artefact assay, plate 1.

0.082	0.087	0.083	0.086	0.211	0.088	0.095	0.085	0.082	0.084	0.082	0.097
0.081	0.098	0.087	0.090	0.111	0.083	0.099	0.082	0.084	0.099	0.087	0.095
0.081	0.086	0.083	0.087	0.090	0.087	0.087	0.152	0.090	0.088	0.085	0.086
0.080	0.088	0.098	0.083	0.146	0.085	0.091	0.085	0.085	0.089	0.084	0.085
0.082	0.085	0.092	0.084	0.091	0.089	0.094	0.083	0.100	0.089	0.085	0.087
0.079	0.081	0.085	0.083	0.123	0.087	0.083	0.079	0.089	0.083	0.083	0.099
0.080	0.097	0.092	0.094	0.192	0.084	0.086	0.082	0.084	0.088	0.086	0.103
0.082	0.080	0.088	0.079	0.087	0.082	0.090	0.079	0.096	0.088	0.084	0.090

Figure 17. Artefact assay control plate 1.

0.675	0.834	0.550	0.651
0.537	0.648	0.596	0.859
0.545	0.595	0.610	0.596
0.527	0.720	0.596	0.515
0.673	0.670	0.579	0.600
0.513	0.565	0.721	0.507
0.579	0.693	0.797	0.477
0.612	0.438	0.620	0.537

Figure 18. Artefact assay control plate 2.

0.096	0.115	0.089	0.105
0.096	0.096	0.091	0.117
0.090	0.092	0.113	0.091
0.095	0.304	0.091	0.086
0.251	0.090	0.086	0.090
0.085	0.147	0.105	0.083
0.085	0.085	0.150	0.081
0.088	0.085	0.098	0.091

Figure 19. Artefact assay, plate 2.

Heat maps of the artefact assay, carried out in two plates, can be seen in figures 15 and 17. The 7 validated hits from the artefact screen are bolded in these figures, while the deionized water controls can be seen in Figures 16 and 18. A scatterplot of this data can also be seen in Figure 19 with validated hits in red. The artefact screen reduced the overall hit rate from 2.54% to 0.14%.

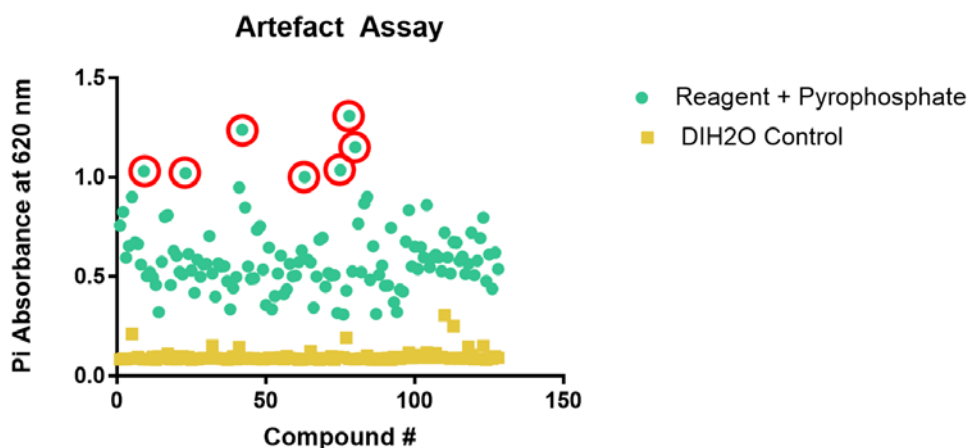


Figure 20. Scatterplot of artefact screen data

After the artefact screen, 7 hits remained. Preliminary *in vitro* data was conducted to further whittle down the list of potential hits to characterize.

#### 4.1.4 *In vivo* screening\*

Two groups of thirty wells were set up containing Müller-Hintin broth, 25µg/mL glucose-6-phosphate, and one of the following: no drug, 1% DMSO, 1% compound in DMSO, or 1024µg/mL fosfomycin. These were inoculated with  $\sim 5 \times 10^5$  CFUs of either VRE WT or C119D bacteria and grown for 24 hours at 35 deg C. As expected, the C119D grew in the presence of

fosfomycin, despite it killing WT. Additionally, 6 compounds inhibited growth of both VRE WT and C119D, which can be seen in Figure 20.

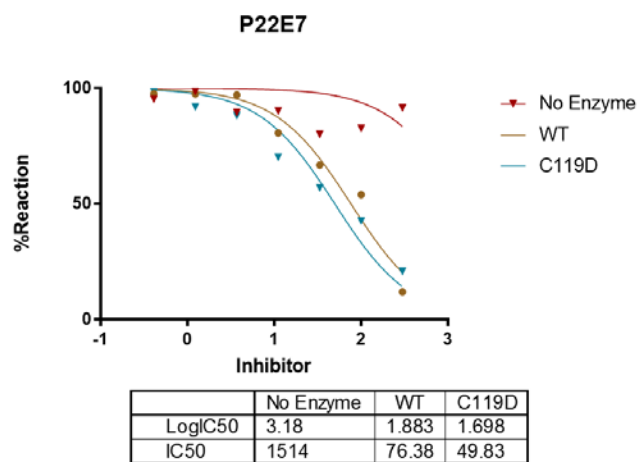
VRE WT					VRE C119D				
1024 Fos	P10C5	P24C4	P34F5	P47G2	1024 Fos	P10C5	P24C4	P34F5	P47G2
No Drug	P10D5	P25F8	P34E7	P49E3	No Drug	P10D5	P25F8	P34E7	P49E3
DMSO	P12B6	P26F10	P34C8	P49H8	DMSO	P12B6	P26F10	P34C8	P49H8
P5B3	P14H5	P29E6	P39F11	P55A8	P5B3	P14H5	P29E6	P39F11	P55A8
P9G9	P14B6	P31A4	P41E4	P62B7	P9G9	P14B6	P31A4	P41E4	P62B7
P9F10	P22E7	P33A7	P46C3	P63B7	P9F10	P22E7	P33A7	P46C3	P63B7

No Growth	Growth
-----------	--------

**Figure 21.** Plate results for *in vivo* screening. Bacterial growth is shown in red, while non-growth is shown in green.

The half maximal inhibitory concentrations (IC<sub>50</sub>s) were determined for these remaining six compounds as well as three previously purchased compounds, and the IC<sub>50</sub>s of the four most promising compounds can be seen in Figures 21 - 24.



**Figure 22.** P22E7 IC<sub>50</sub> curve.

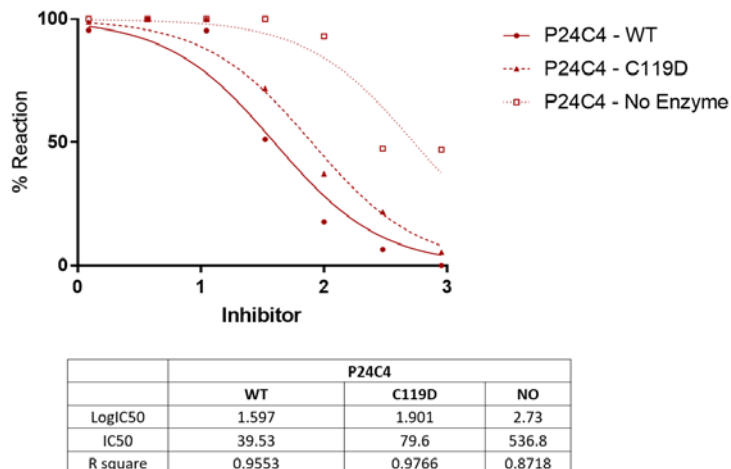


**Figure 23.** P24C4 IC<sub>50</sub> curve.

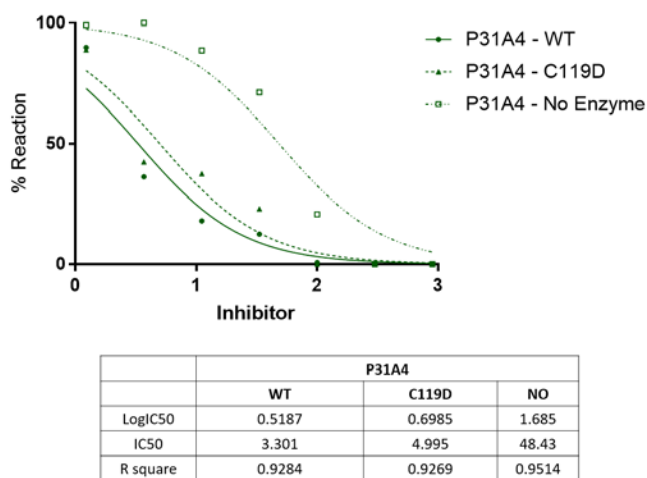


**Figure 24.** P22E7 IC<sub>50</sub> curve.

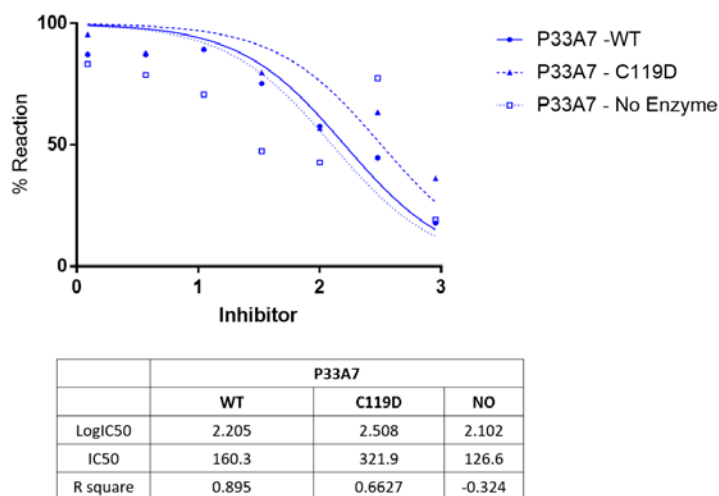


**Figure 25.** P33A7 IC<sub>50</sub> curve.

\*The *in vivo* and IC<sub>50</sub> data in this section was provided courtesy of Adam Tomich in the Sluis-Cremer Lab.

Compounds P24C4 and P31A4 had the lowest IC<sub>50</sub> values at 39.53 and 3.301 respectively. P22E7 also had a promising IC<sub>50</sub> curve despite its higher IC<sub>50</sub> value. These three compounds were selected for further consideration. The hit rate for each stage of high-

throughput screening can be seen in Table 1. After these hits were validated, we proceeded to further characterize these compounds in bacteria and in human cell lines.

**Table 1.** High-throughput screen hit rate.

			<b>Hit Rate</b>
<b>Total # Compounds:</b>	5040		
<b>Primary Screen WT Hits:</b>	910		18.06%
<b>Secondary Screen WT Hits:</b>	775		15.38%
<b>Overlap WT + C119D hits:</b>	128		2.54%
<b>Artefact Screen hits:</b>	7		0.14%
<b>Preliminary <i>in vitro</i> hits:</b>	3		0.060%

## 4.2 AIM 2: INHIBITOR CHARACTERIZATION

### 4.2.1 MIC Assay

To determine the MICs of each compound, VRE WT and C119D were used as bacterial strains of interest along with commercially available strains of *E. coli* and *S. aureus* for gram-negative and gram-positive controls, respectively. Two trials were performed with each MIC assay; results from one trial of each compound are shown for brevity in figures 25 – 27, and tables 2 – 4.

Plate 1A		1	2	3	4	5	6	7	8	9	10	11	12
Fosfomycin (ug/mL)		0	1	2	4	8	16	32	64	128	256	512	1024
P22E7 (ug/mL)		0.0	0.1	0.2	0.4	0.9	1.8	3.5	7.0	14.0	28.0	56.0	112.0
A	VRE WT + Fosfomycin												
B	VRE WT + P22E7												
C	VRE WT + DMSO												
D	C119D + Fosfomycin												
E	C119D + P22E7												
F	C119D + DMSO												
No Growth													
Growth													

Plate 1B		1	2	3	4	5	6	7	8	9	10	11	12
Fosfomycin (ug/mL)		0	1	2	4	8	16	32	64	128	256	512	1024
P22E7 (ug/mL)		0.0	0.1	0.2	0.4	0.9	1.8	3.5	7.0	14.0	28.0	56.0	112.0
A	SA 25923 + Fosfomycin												
B	SA 25923 + P22E7												
C	SA 25923 + DMSO												
D	EC 25922 + Fosfomycin												
E	EC 25922 + P22E7												
F	EC 25922 + DMSO												
No Growth													
Growth													

Figure 26. Representative MIC results for compound P22E7.

In Figure 26, VRE WT bacteria is susceptible to fosfomycin, while the C119D bacteria is not. P22E7 kills both VRE WT and C119D bacterial strains, and kills *S. aureus*, but not *E. coli*.

Plate 1A		1	2	3	4	5	6	7	8	9	10	11	12
Fosfomycin (ug/mL)		0	1	2	4	8	16	32	64	128	256	512	1024
P24C4 (ug/mL)		0	0.08	0.16	0.31	0.63	1.25	2.5	5	10	20	40	80
A	VRE WT + Fosfomycin												
B	VRE WT + P24C4												
C	VRE WT + DMSO												
D	C119D + Fosfomycin												
E	C119D + P24C4												
F	C119D + DMSO												
No Growth													
Growth													

Plate 1B		1	2	3	4	5	6	7	8	9	10	11	12
Fosfomycin (ug/mL)		0	1	2	4	8	16	32	64	128	256	512	1024
P24C4 (ug/mL)		0	0.08	0.16	0.31	0.63	1.25	2.5	5	10	20	40	80
A	SA 25923 + Fosfomycin												
B	SA 25923 + P24C4												
C	SA 25923 + DMSO												
D	EC 25922 + Fosfomycin												
E	EC 25922 + P24C4												
F	EC 25922 + DMSO												
No Growth													
Growth													

Figure 27. Representative MIC results for compound P24C4.

In Figure 27, VRE WT is again susceptible to fosfomycin, while VRE C119D is not. P24C4 killed VRE WT at a higher dose than fosfomycin, and also killed VRE C119D bacteria. While P24C4 killed *S. aureus*, it did not affect *E. coli*.

Plate 1A		1	2	3	4	5	6	7	8	9	10	11	12
Fosfomycin (ug/mL)		0	1	2	4	8	16	32	64	128	256	512	1024
P31A4 (ug/mL)		0	0.07	0.14	0.27	0.55	1.09	2.2	4	8.8	18	35	70
A	VRE WT + Fosfomycin												
B	VRE WT + P31A4												
C	VRE WT + DMSO												
D	C119D + Fosfomycin												
E	C119D + P31A4												
F	C119D + DMSO												
Plate 1B		1	2	3	4	5	6	7	8	9	10	11	12
Fosfomycin (ug/mL)		0	1	2	4	8	16	32	64	128	256	512	1024
P31A4 (ug/mL)		0	0.07	0.14	0.27	0.55	1.09	2.2	4	8.8	18	35	70
A	SA 25923 + Fosfomycin												
B	SA 25923 + P31A4												
C	SA 25923 + DMSO												
D	EC 25922 + Fosfomycin												
E	EC 25922 + P31A4												
F	EC 25922 + DMSO												
	No Growth												
	Growth												

**Figure 28.** Representative MIC results for compound P31A4.

In Figure 28, compound P31A4 is effective against both VRE WT and C119D bacteria, and like the other two compounds is effective against gram positive *S. Aureus* while not being effective against gram negative *E. coli*. The average MIC values for P22E7 (Table 2) are comparable in both VRE WT and C119D bacterial strains at 0.1-0.2µg/mL, while the MIC in *S. aureus* is much higher for P22E7 than for fosfomycin.

**Table 2.** P22E7 average MIC values.

Avg Drug (µg/mL)	Strain			
	VRE WT	C119D	<i>S. aureus</i>	<i>E. coli</i>
Fosfomycin	64	>1024	2-4	1
P22E7	0.1-0.2	0.1-0.2	0.1	>112

The average MIC values for P24C4 (Table 3) are about the same in VRE WT, C119D, and *S. aureus* bacteria, while exceeding the maximum inhibitor concentration in *E. coli*. Fosfomycin has lower MIC values than P24C4 in both *S. aureus* and *E. coli* strains.

**Table 3.** P24C4 average MIC values.

Avg Drug (µg/mL)	Strain			
	VRE WT	C119D	<i>S. aureus</i>	<i>E. coli</i>
Fosfomycin	128	>1024	1-8	1
P24C4	20	10-20	20	>80

The average MIC values for P31A4 (Table 4) were very similar in VRE WT, C119D, and *S. aureus*, while the P31A4 MIC was much higher in *E. coli* than the fosfomycin MIC for this strain.

**Table 4.** P31A4 average MIC values.

Avg Drug (µg/mL)	Strain			
	VRE WT	C119D	<i>S. aureus</i>	<i>E. coli</i>
Fosfomycin	128	>1024	1-2	1
P31A4	0.55	0.55	0.55-1.09	>70

## 4.2.2 Toxicity Assays

After the MIC values for each compound were determined, toxicity assays were performed using two cell lines: HeLa (a cervical cancer cell line) and 293T HEK (a human kidney cell line). Compounds were incubated with each cell line at varying concentrations above and below respective MIC values. Figures 29-36 illustrate percentage of cell viability vs an array of concentrations of a given compound.

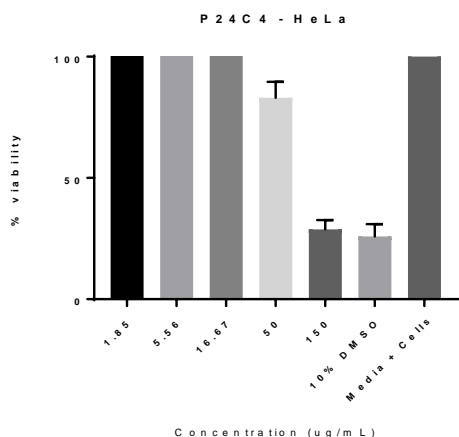


**Figure 30.** HeLa incubated with [P24C4].

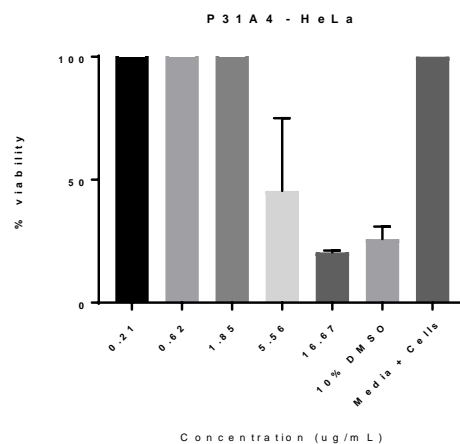


**Figure 29.** HeLa incubated with [P31A4].

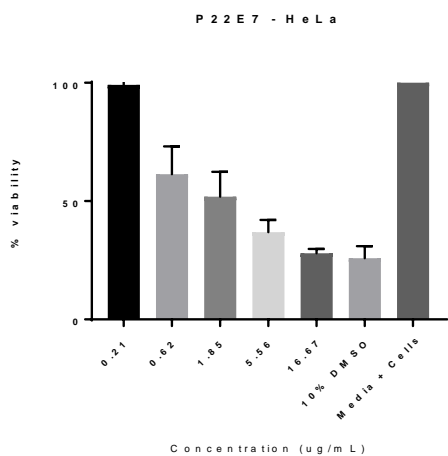


**Figure 31.** HeLa incubated with [P22E7].

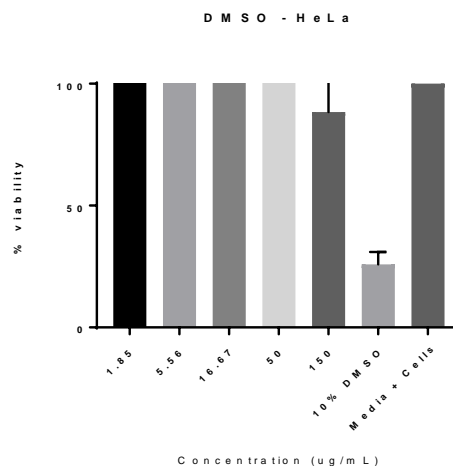


**Figure 32.** HeLa incubated with DMSO controls.

When HeLa cells were incubated with varying concentrations of P24C4 (ranging from 1.85  $\mu\text{g}/\text{mL}$  to 150  $\mu\text{g}/\text{mL}$ ), cells remained close to 100% viable until incubated with a dose of 50.00  $\mu\text{g}/\text{mL}$  inhibitor, when the viability decreased to approximately 75%. For cells incubated with the same range of concentrations for P31A4, the percent viability dropped below the DMSO control for 16.67  $\mu\text{g}/\text{mL}$  inhibitor. The P22E7 inhibitor resulted in the lowest percentage of cell viability across the board, with the most concentrated dose rivaling the cell viability of the 10% DMSO control. The 10% DMSO controls in each assay all resulted in significantly low cell viability for both cell lines. The percentage of cell viability for cells incubated with the varying lower concentrations of DMSO were approximately 100%, except for the 10% DMSO treatment which resulted in approximately 10% of cell viability.

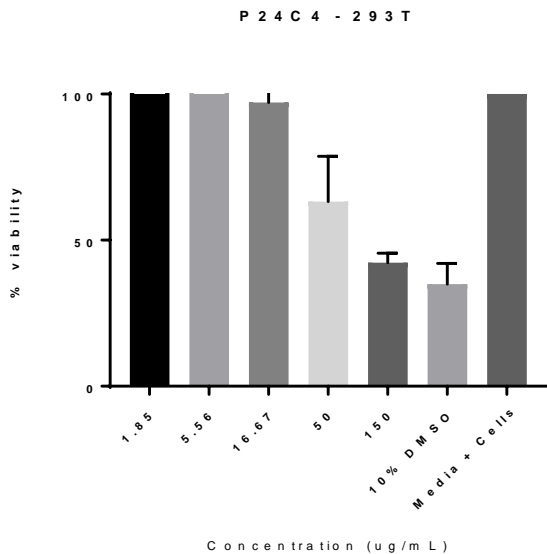


**Figure 34.** 293T incubated with [P24C4].

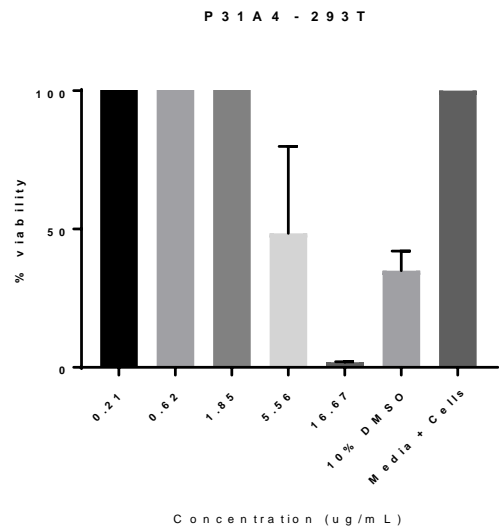


**Figure 33.** 293T incubated with [P31A4].

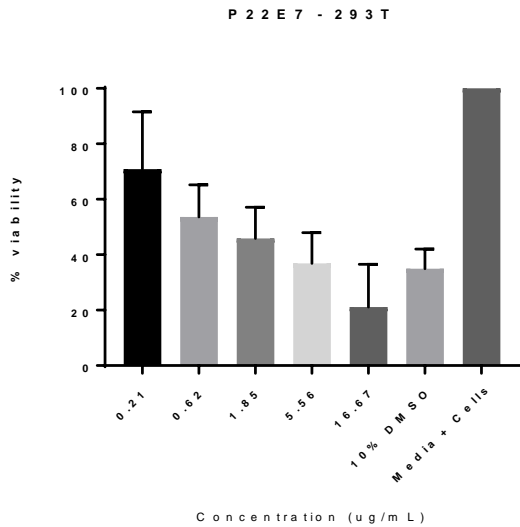


**Figure 36.** 293T incubated with [P22E7].

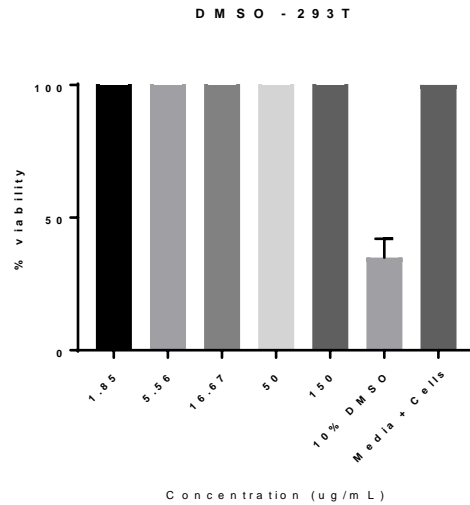


**Figure 35.** 293T incubated with DMSO controls.

When 293T cells were incubated with the same range of concentrations of P24C4, cells again remained nearly 100% viable until incubated with a dose of 50.00 $\mu$ g/mL, where the cell viability dropped to approximately 75%. When incubated with P31A4, cell viability dropped significantly below the viability of the 10% DMSO control when incubated with 16.67 $\mu$ g/mL. For the cells incubated with P22E7, there is a decrease of cell viability in a dose-dependent fashion as concentration of P22E7 is increased. Again, cell viability was about 100% for cells incubated with DMSO controls at these same concentrations, with the exception of 10% DMSO where cells had about a 20% viability. All cells incubated with varying concentrations of DMSO demonstrated a cell viability of nearly 100% with the exception of the 10% DMSO control, which hovered around 25%.

### 4.2.3 Selectivity Indexes

A further value which may help elucidate therapeutic potential for these drugs is the selectivity index. Selectivity indexes (SIs) were calculated from the MIC assays and toxicity assays ( $SI = CC_{50}/MIC$ ), and can be seen below in Table 5.

**Table 5.** Inhibitor selectivity indexes.

<b>Inhibitor</b>	<b>Selectivity Index</b>
P24C4	5
P31A4	10.9
P22E7	9.25-18.5

## 5.0 DISCUSSION

### 5.1 ENZYME PURIFICATION

Weak bands for TB MurA enzyme indicate little presence of TB MurA, which suggests a low yield from protein purifications. The project subsequently proceeded with only VRE WT and VRE C119D MurA enzymes. Because one of the potential applications of a MurA inhibitor may be to treat bacterial infections caused by *M. tuberculosis*, it would be of interest to purify TB MurA and screen it against a drug library in a similar manner.

### 5.2 PRIMARY AND SECONDARY SCREENS

Positive and negative enzyme controls were averaged in data analysis. Any outlier wells were dropped from data analysis, though this incident only occurred a handful of times over the hundreds of plates used in primary and secondary screens.

As a general trend, there were significantly more hits identified in the primary screen for VRE WT MurA than for VRE C119D. The stark difference in number of initial hits may be due to the substitution from cysteine to aspartic acid in the active site of the MurA enzyme. Cysteine is a small, polar, amino acid, while aspartic acid is a much larger and acidic residue, so we speculate that differences in steric interactions may have resulted in the discrepancy between

numbers of initial hits. In addition, raising of the 70% inhibition threshold would have resulted in a smaller number of hits.

It is also important to mention that the TimTec® ApexScreen drug library used in the project has also been used in other experiments within the Sluis-Cremer lab. Because the amount of drug in each well of the library may have been depleted in some cases, a decreased amount of some drugs may have been deposited in some of the assay plates, resulting in potential false-negative hits. Careful pipetting technique was implemented to minimize determination of false-negative hits.

### **5.3 ARTEFACT SCREEN**

The threshold for validation in the artefact screen was determined to be any spectrophotometer reading above 1.000, though we recognize that a lower threshold would have validated more hits to further analyze. Following up with some of the hits in the artefact screen at a slightly lower threshold may be of interest to others looking to identify MurA inhibitors.

### **5.4 MIC ASSAYS**

Controls for the MIC assays are unremarkable; fosfomycin is active against WT but not C119D, which is expected as the C119D bacterial strain does not contain fosfomycin's target cysteine residue in the MurA active site. P22E7 results suggest that this inhibitor may require a smaller dose to kill bacteria than fosfomycin, but its activity against *S. aureus* coupled with its

ineffectiveness against *E. coli* suggest gram-positive specificity. P22E7 was also active against both VRE WT and C119D bacteria which strongly implies a different mechanism of action than fosfomycin.

P24C4 results suggest a comparable dose required to kill VRE WT bacteria, and P24C4 is also effective against C119D bacteria, which again suggests a different mechanism of action of MurA inhibition than fosfomycin. P31A4 required a smaller dose than fosfomycin to kill VRE WT bacteria, and was also effective against VRE C119D. Both P24C4 and P31A4, like P22E7, appear to have gram-positive antibacterial specificity, which would render them inactive against gram-negative pathogens such as bacterial infections caused by *M. tuberculosis*. However, results seemed promising enough to proceed with toxicity assays.

## **5.5 TOXICITY ASSAYS**

### **5.5.1 HeLa cells**

HeLa cells were chosen due to their ubiquitous nature, as well as their price and ability to grow rapidly and reliably as a human cell line. P24C4 appeared to become toxic starting at a dose of 50 $\mu$ g/mL, while its highest MIC was determined to be about 20 $\mu$ g/mL, so this drop in cell viability may not suggest overwhelming toxicity if tested *in vivo*. Similarly, P31A4 experienced a drop in cell viability at 5.56 $\mu$ g/mL while its highest MIC value was 1.09 $\mu$ g/mL. P22E7 however appeared to be toxic at all doses, indicating that administration of an effective dose to kill a given bacterial infection may also be incompatible with life of the organism. P22E7 is

again probably too toxic to be usefully utilized in treatment of human cells, but more studies should be conducted to further elucidate its potential.

### **5.5.2 293T cells**

293T cells were selected as a secondary cell line because they are a human kidney cell line, which is a likely a better model for illustrating drug toxicity than HeLa, a gynecological cervical cancer cell line. Because P24C4 treated 293T cells appeared to have a similar viability as the HeLa cell line, P24C4 is likely a promising MurA inhibitor to further investigate. P31A4 appears slightly less so, with cell viability dropping at 5.56 $\mu$ g/mL, and P22E7 was again very toxic to cells at any concentration.

Overall, further toxicity assays are required to determine a therapeutic index for these three inhibitors. However, based on these preliminary findings, it appears that P24C4 and P31A4 may be promising inhibitors to further characterize while P22E7 is likely too toxic to be a useful antimicrobial agent in this context. Additionally, studies examining route of drug administration and optimization will also need to be conducted to further elucidate interactions between these inhibitors, bacteria, and host cells.

### **5.5.3 Selectivity Indexes**

The selectivity indexes for the three inhibitors were extremely low (5, 10.9, and 9.25-18.5 for P24C4, P31A4, and P22E7, respectively). Typically, drugs used clinically will have selectivity index values well over 100. These low SI values further indicate that there is likely not a large

window for therapeutic use of these inhibitors in which they can kill the pathogen without killing host cells.

## 6.0 CONCLUSIONS

In conclusion, we developed a high-throughput screening assay to screen purified MurA enzyme against the TimTec® ApexScreen library, with the goal of identifying MurA inhibitors with a mechanism of action different than fosfomycin. We purified two MurA variants, VRE WT MurA, and VRE C119D MurA. These enzymes were both screen concurrently against the TimTec® Apexscreen library, and also screened for artefacts. The screens along with preliminary *in vitro* data suggested three promising candidates: P22E7, P24C4, and P31A4.

MIC assay data illustrated that all three of these candidates are gram-positive specific, suggesting that these compounds would not be suitable to develop against pathogens such as *M. tuberculosis*. However, this result is not surprising because gram positive organisms tend to be easier to kill, due to their thicker layer of peptidoglycan within the outer membrane of the bacterial cell. Toxicity assays conducted in both HeLa and 293T cell lines suggest that compound P22E7 may be too toxic in human cells, while P24C4 and P31A4 require more studies to determine an accurate therapeutic index.

Moving forward, compounds P24C4 and P31A4 should be further characterized to determine whether they are suitable to be used as clinical antimicrobial agents.

## 7.0 PUBLIC HEALTH RELEVANCE

Antimicrobial resistance delays treatment of drug-resistant infections, increases the duration of infection, and expands the timeframe through which resistant microorganisms can spread to others. From a public health perspective, the patient remains a reservoir of infection for a longer period of time, putting community and health care workers at greater risk (48). Aside from complicating the treatment of infection, antibiotic resistance is associated with increased morbidity and mortality and significant economic loss, often resulting in prolonged hospital stays and thus greater financial cost to the hospital, patient, and society. The risk of these adverse events has been shown to be greater with drug resistant infections compared to their drug-susceptible counterparts even when adjusting for co-morbidities (49).

The data presented in this body of work reflects the popular strategy in recent years to re-evaluate and expand the use of older antimicrobials to treat a broader range of drug-resistant infections. The compound identified in this work offers a potential inhibitor that may be developed into a therapeutic agent and thus expand the use of fosfomycin in a clinical setting. With the ability to treat both gram-negative and gram-positive infections, such an agent can be used to treat a broad range of potentially resistant bacterial infections, resulting in maximum public health impact.

## BIBLIOGRAPHY

1. Fleming A. 1929. On the Antibacterial Action of Cultures of a *Penicillium*, with Special Reference to their Use in the Isolation of *B. influenzae*. *British journal of experimental pathology* 10:226-236.
2. Adedeji WA. 2016. The Treasure Called Antibiotics. *Annals of Ibadan Postgraduate Medicine* 14:56-57.
3. Ligon BL. 2004. Penicillin: its discovery and early development. *Seminars in Pediatric Infectious Diseases* 15:52-57.
4. Lewis K. 2013. Platforms for antibiotic discovery. *Nat Rev Drug Discov* 12:371-87.
5. Singh V, Haque S, Singh H, Verma J, Vibha K, Singh R, Jawed A, Tripathi CKM. 2016. Isolation, Screening, and Identification of Novel Isolates of Actinomycetes from India for Antimicrobial Applications. *Frontiers in Microbiology* 7:1921.
6. Davies J. 2006. Where have All the Antibiotics Gone? *The Canadian Journal of Infectious Diseases & Medical Microbiology* 17:287-290.
7. Aminov RI. 2010. A Brief History of the Antibiotic Era: Lessons Learned and Challenges for the Future. *Frontiers in Microbiology* 1:134.
8. Armstrong GL, Conn LA, Pinner RW. 1999. Trends in infectious disease mortality in the United States during the 20th century. *Jama* 281:61-6.
9. Anonymous. National vital statistics reports : from the Centers for Disease Control and Prevention, National Center for Health Statistics, National Vital Statistics System.
10. Lobanovska M, Pilla G. 2017. Penicillin's Discovery and Antibiotic Resistance: Lessons for the Future? *The Yale Journal of Biology and Medicine* 90:135-145.
11. Breslow L. 1990. The future of public health: prospects in the United States for the 1990s. *Annu Rev Public Health* 11:1-28.
12. Abraham EP, Chain E. 1988. An enzyme from bacteria able to destroy penicillin. 1940. *Rev Infect Dis* 10:677-8.
13. Munita JM, Arias CA. 2016. Mechanisms of Antibiotic Resistance. *Microbiology spectrum* 4:10.1128/microbiolspec.VMBF-0016-2015.
14. Spellberg B, Gilbert DN. 2014. The Future of Antibiotics and Resistance: A Tribute to a Career of Leadership by John Bartlett. *Clinical Infectious Diseases: An Official Publication of the Infectious Diseases Society of America* 59:S71-S75.
15. Hawkey PM. 1998. The origins and molecular basis of antibiotic resistance. *BMJ : British Medical Journal* 317:657-660.
16. Imperial ICVJ, Ibana JA. 2016. Addressing the Antibiotic Resistance Problem with Probiotics: Reducing the Risk of Its Double-Edged Sword Effect. *Frontiers in Microbiology* 7:1983.
17. Anonymous. 2013. The antibiotic alarm. *Nature* 495:141.

18. Lushniak BD. 2014. Antibiotic resistance: a public health crisis. *Public Health Rep* 129:314-6.
19. Administration FaD. 2014. Summary Report On Antimicrobials Sold or Distributed for Use in Food-Producing Animals.
20. Martin MJ, Thottathil SE, Newman TB. 2015. Antibiotics Overuse in Animal Agriculture: A Call to Action for Health Care Providers. *American Journal of Public Health* 105:2409-2410.
21. Van Boeckel TP, Brower C, Gilbert M, Grenfell BT, Levin SA, Robinson TP, Teillant A, Laxminarayan R. 2015. Global trends in antimicrobial use in food animals. *Proceedings of the National Academy of Sciences of the United States of America* 112:5649-5654.
22. Ventola CL. 2015. The Antibiotic Resistance Crisis: Part 1: Causes and Threats. *Pharmacy and Therapeutics* 40:277-283.
23. Piddock LJ. 2012. The crisis of no new antibiotics--what is the way forward? *Lancet Infect Dis* 12:249-53.
24. Falagas ME, Kastoris AC, Karageorgopoulos DE, Rafailidis PI. 2009. Fosfomycin for the treatment of infections caused by multidrug-resistant non-fermenting Gram-negative bacilli: a systematic review of microbiological, animal and clinical studies. *Int J Antimicrob Agents* 34:111-20.
25. Falagas ME, Vouloumanou EK, Samonis G, Vardakas KZ. 2016. Fosfomycin. *Clinical Microbiology Reviews* 29:321-347.
26. Organization TWH. 2017. Antibacterial Agents in Clinical Development: An analysis of the antibacterial clinical development pipeline, including tuberculosis.,
27. Sulis G, Roggi A, Matteelli A, Raviglione MC. 2014. Tuberculosis: Epidemiology and Control. *Mediterranean Journal of Hematology and Infectious Diseases* 6:e2014070.
28. Velayati AA, Farnia P, Farahbod AM. 2016. Overview of drug-resistant tuberculosis worldwide. *Int J Mycobacteriol* 5 Suppl 1:S161.
29. Munita JM, Bayer AS, Arias CA. 2015. Evolving Resistance Among Gram-positive Pathogens. *Clinical Infectious Diseases: An Official Publication of the Infectious Diseases Society of America* 61:S48-S57.
30. Rice LB. 2006. Antimicrobial resistance in gram-positive bacteria. *Am J Infect Control* 34:S11-9; discussion S64-73.
31. Hendlin D, Stapley EO, Jackson M, Wallick H, Miller AK, Wolf FJ, Miller TW, Chaiet L, Kahan FM, Foltz EL, Woodruff HB, Mata JM, Hernandez S, Mochales S. 1969. Phosphonomycin, a new antibiotic produced by strains of streptomyces. *Science* 166:122-3.
32. Docobo-Perez F, Drusano GL, Johnson A, Goodwin J, Whalley S, Ramos-Martin V, Ballesterro-Tellez M, Rodriguez-Martinez JM, Conejo MC, van Guilder M, Rodriguez-Bano J, Pascual A, Hope WW. 2015. Pharmacodynamics of fosfomycin: insights into clinical use for antimicrobial resistance. *Antimicrob Agents Chemother* 59:5602-10.
33. Picozzi SCM, Casellato S, Rossini M, Paola G, Tejada M, Costa E, Carmignani L. 2014. Extended-spectrum beta-lactamase-positive *Escherichia coli* causing complicated upper urinary tract infection: Urologist should act in time. *Urology Annals* 6:107-112.
34. Dijkmans AC, Zacarias NVO, Burggraaf J, Mouton JW, Wilms EB, van Nieuwkoop C, Touw DJ, Stevens J, Kamerling IMC. 2017. Fosfomycin: Pharmacological, Clinical and Future Perspectives. *Antibiotics (Basel)* 6.

35. Michalopoulos A, Vartzili S, Rafailidis P, Chalevelakis G, Damala M, Falagas ME. 2010. Intravenous fosfomycin for the treatment of nosocomial infections caused by carbapenem-resistant *Klebsiella pneumoniae* in critically ill patients: a prospective evaluation. *Clin Microbiol Infect* 16:184-6.
36. Xu YJ, Quan JJ, Shi KR, Yu YS. 2018. [Mechanisms of fosfomycin resistance of extended-spectrum beta-lactamases-producing *Escherichia coli* and *Klebsiella pneumoniae*]. *Zhonghua Yi Xue Za Zhi* 98:122-126.
37. Patel B, Patel K, Shetty A, Soman R, Rodrigues C. 2017. Fosfomycin Susceptibility in Urinary Tract Enterobacteriaceae. *J Assoc Physicians India* 65:14-16.
38. Klontz EH, Tomich AD, Gunther S, Lemkul JA, Deredge D, Silverstein Z, Shaw JF, McElheny C, Doi Y, Wintrobe PL, MacKerell AD, Jr., Sluis-Cremer N, Sundberg EJ. 2017. Structure and Dynamics of FosA-Mediated Fosfomycin Resistance in *Klebsiella pneumoniae* and *Escherichia coli*. *Antimicrob Agents Chemother* 61.
39. Sastry S, Doi Y. 2016. Fosfomycin: Resurgence of An Old Companion. *Journal of infection and chemotherapy : official journal of the Japan Society of Chemotherapy* 22:273-280.
40. Guo Y, Tomich AD, McElheny CL, Cooper VS, Tait-Kamradt A, Wang M, Hu F, Rice LB, Sluis-Cremer N, Doi Y. 2017. High-Level Fosfomycin Resistance in Vancomycin-Resistant *Enterococcus faecium*. *Emerging Infectious Diseases* 23:1902-1904.
41. Silver LL. 2017. Fosfomycin: Mechanism and Resistance. *Cold Spring Harb Perspect Med* 7.
42. Nikolaidis I, Favini-Stabile S, Dessen A. 2014. Resistance to antibiotics targeted to the bacterial cell wall. *Protein Science : A Publication of the Protein Society* 23:243-259.
43. Marblestone JG, Edavettal SC, Lim Y, Lim P, Zuo X, Butt TR. 2006. Comparison of SUMO fusion technology with traditional gene fusion systems: Enhanced expression and solubility with SUMO. *Protein Science : A Publication of the Protein Society* 15:182-189.
44. Pollastri MP. 2010. Overview on the Rule of Five. *Curr Protoc Pharmacol Chapter 9:Unit 9.12*.
45. Yang JJ, Ursu O, Lipinski CA, Sklar LA, Oprea TI, Bologa CG. 2016. Badapple: promiscuity patterns from noisy evidence. *J Cheminform* 8:29.
46. Andrews JM. 2001. Determination of minimum inhibitory concentrations. *J Antimicrob Chemother* 48 Suppl 1:5-16.
47. Sasahara H, Sugiyama K, Tsukaguchi M, Isogai K, Toyama A, Satoh H, Saitoh K, Nakagawa Y, Takahashi K, Tanaka S, Onda K, Hirano T. 2013. Comparison of the Pharmacological Efficacies of Immunosuppressive Drugs Evaluated by the ATP Production and Mitochondrial Activity in Human Lymphocytes. *Cell Medicine* 6:39-45.
48. Jindal AK, Pandya K, Khan ID. 2015. Antimicrobial resistance: A public health challenge. *Medical Journal, Armed Forces India* 71:178-181.
49. Mulvey MR, Simor AE. 2009. Antimicrobial resistance in hospitals: How concerned should we be? *CMAJ : Canadian Medical Association Journal* 180:408-415.